Probabilistic multimodal map-matching with rich smartphone data

Jingmin Chen * Michel Bierlaire *

June 18, 2012

Report TRANSP-OR 120618
Transport and Mobility Laboratory
Ecole Polytechnique Fédérale de Lausanne
transp-or.epfl.ch

Abstract

This paper proposes a probabilistic method that infers the transport modes and the physical path of trips from smartphone data that were recorded during travels. This method synthesizes multiple kinds of data from smartphone sensors which provide relevant location or transport mode information: GPS, Bluetooth, and Accelerometer. The method is based on a smartphone measurement model that calculates the likelihood of observing the smartphone data in the multimodal transport network. The output of this probabilistic method is a set of candidate true paths, and the probability of each path being the true one. The transport mode used on each arc is also inferred. Numerical experiments include map visualizations of some example trips, and an analysis on the performance of the transport mode inference.

Keywords: multimodal map-matching, transport mode inference, smartphone data, GPS, Bluetooth, acceleration

1 Introduction

Embedded with various sensors, such as GPS and accelerometer, smartphones can be utilized to understand the users' context. They become popular as data collection tools in studying mobility patterns and transportation network performances. For examples, González,

*Transport and Mobility Laboratory, Ecole Polytechnique Fédérale de Lausanne, CH-1015 Lausanne, Switzerland

Hidalgo & Barabási (2008) learn from 100,000 mobile phone users' positions that human mobility has a high degree of spatial and temporal patterns; Tam & Lam (2008) use vehicles' GPS data to estimate road travel time; Bierlaire, Chen & Newman (2010) use smartphone GPS data to model individual route choice behavior. As both information receiver and context monitor, the smartphones can also be used as a platform to learn users' behavior responses to the transportation information services.

In order to provide useful information for transportation studies, the mobility history has to be recovered from the raw smartphone data. Information such as the transport modes and the paths of trips need to be learnt. Due to low-cost sensors' poor performances and various practical constraints, the smartphone data are usually sparse and inaccurate. For example, data recording interval for GPS is set to be quit large (10 seconds), and the smartphone GPS data are not accurate (Bierlaire et al. 2010). Moreover, retrieving and synthesizing information from various sensors are also challenging.

Traditionally, transport mode inference and physical path detection (a.k.a map-matching) are applied to GPS data only, and consist of two steps (e.g. Schuessler & Axhausen 2009a):

1. Split the data into multiple unimodal segments, each of which representing a continuous travel without mode change or vehicle change.
2. Do map-matching and transport mode inference for each segment independently.

This two step technique poses a high risk of yielding wrong results, because potentially wrong segmentations in the first step are not recoverable. Many algorithms assume that walking is necessary for a transition between different modes, and they rely on dense GPS data (1 second interval) to detect the mode (e.g. Zheng, Li, Chen, Xie & Ma 2008, Zhang, Dalyot, Eggert, Sester, Ikg, Hannover & De 2008, Schuessler & Axhausen 2009a). The validity of this assumption is questionable, especially for smartphone data, because GPS data could be missing due to the unavailability of the GPS signal while walking indoor. Moreover, due to the sparsity of the GPS data on a smartphone, they may not provide sufficient information for a proper segmentation and mode inference.

In this paper, a novel algorithm is proposed to overcome these drawbacks. The data collected from a trip do not need to be segmented. The algorithm infers the physical path and the transport mode of each road simultaneously. This algorithm is called as *probabilistic multimodal map-matching*:

- Multimodal, because the output is a set of multimodal paths. Each arc on a path is associated with a specific transport mode. The transport modes on different arcs may differ (see Section 2 for the definition and an example of multimodal path).
- Probabilistic, because the algorithm generates a set of candidate paths, each of which associated with a probability to be the true one.

Rich information available from multiple smartphone sensors is exploited in this algorithm. Smartphones, e.g. iPhone and Nokia 95, are usually embedded with a 3-axis accelerometer with $\pm 2G$ sensitivity. Researches have found that acceleration data from accelerometers are useful in recognizing the motion status of the phone carrier (e.g. Reddy, Burke, Estrin, Hansen & Srivastava 2009, Kwapisz, Weiss & Moore 2010). Moreover, the BT sensor also provides valuable information about the smartphone's context. For example, the BT sensor detects more nearby BT devices in a public transport environment than in a private mode. We propose a framework that can exploit any kind of data if it provides information about the location or the transport mode. Although only data from GPS, BT and ACCEL are studied in this paper, the method can be extended to any type of sensor that provides contextual information, such as gyroscope.

This algorithm is an extension of the unimodal map-matching algorithm proposed by Bierlaire et al. (2010). A probabilistic measurement model is derived for each sensor to capture the data generation process. (Section 3). An integrated smartphone measurement model is constructed to integrate all sensor models in a unified framework. The smartphone measurement model calculates the likelihood of observing the smartphone measurements on a multimodal path (Section 4). Then, a multimodal map-matching algorithm is proposed to generate candidate paths from the smartphone data and a multimodal network (Section 5). The probability for each path being the true one is calculated from the smartphone measurement model. Numerical experiments are illustrated in section 6. Finally, discussions and conclusions are given in section 7.

2 Smartphone data and transport networks

The method proposed in this paper rely on two types of inputs: a model of the transport networks, and the smartphone data collected during travels.

2.1 Multimodal transport network and multimodal path

A network is a directed graph $G = \{N, A\}$, which is composed of a set of arcs A that connect their nodes N. In a transport network, each arc $a \in A$ represents a road segment or a rail track segment, and accommodates one particular transport mode m. Thus, a road that can be traveled with bus and car, is represented by two arcs. A unimodal transport network G_m contains only arcs with the same transport mode m. In this paper, we assume that the smartphone data are recorded while the carrier is traveling on a multimodal transport network. A multimodal transport network is represented by a union of several unimodal transport networks, and virtual arcs that connect them. A virtual arc is associated with a change of transport mode, and connects two nodes belonging to two different unimodal networks but associated with the same geographical location. This paper models urban transport modes, private walk, bike, car, and public bus, metro.

A position $\mathbf{x} = (x, m)$ in a multimodal network is characterized by horizontal coordinates $x = (x_{lat}, x_{lon})$ consisting of latitude and longitude, and transport mode $m \in \{\text{walk}, \text{bike}, \text{car}, \text{bus}, \text{metro}\}$. A path is an ordered list of connected arcs. A multimodal path p is a path in a multimodal network [1]. A multimodal path may contain only one single mode or several different modes. Figure 1 gives an example of a multimodal network with two unimodal networks (bus and walk), and a multimodal path. For the sake of clarity of the drawing, the arcs are represented bidirectional, and the directions are not drawn. Dashed lines represent virtual arcs that connect two unimodal networks. A multimodal path with direction starts from the bus network, and change to walk via a virtual arc connecting $\mathbf{x}_c^- = (x_c, bus)$ and $\mathbf{x}_c^+ = (x_c, \text{walk})$, where x_c denotes the coordinates of the mode change location.

A free and open source map service, *OpenStreetMap.org* (OSM), is used as the source of the transport networks data. In this database, the transport mode accessibility on each road is specified and the public transport lines are also available. The OSM data structure is only designed for visualization, and the PT network data have to be preprocessed for routing and map-matching usages. The metro stops are sometimes disconnected from other networks. We assume that people can access/egress them by walking from/to the nearest nodes, and create walking arcs to connect metro stops to the 5 nearest nodes. For the sake of simplicity, each arc is created as a straight line.

[1] By default , "path" refers to "multimodal path" in this paper; "physical path" refers to a path without mode information.

2.2 Smartphone data

Since 2009, the Nokia Research Center in Lausanne has been continuously collecting data from 200 smartphones for 2 years (Kiukkonen, Blom, Dousse, Gatica-Perez & Laurila 2010). These data include GPS, acceleration (ACCEL), nearby WIFI spots, nearby Bluetooth (BT) devices, etc. Smartphone data being studied in this paper are collected with a dedicated data recording application (APP) developed by Nokia, Ecole Polytechnique Fédérale de Lausanne, and IDIAP Switzerland. When a sensor is activated, the APP triggers sensor reading events periodically and logs the data. The availability of data is also subject to practical constraints. For example, GPS data are observed only if the GPS signal is available. And sometimes, the user may turn off the BT sensor. The raw sensor readings, e.g. a list of MAC addresses of nearby BT devices, are usually not ready to be used directly. So useful measurements need to be extracted from the raw data. This process is termed feature extraction in pattern recognition literature. The mechanism of reading sensors, and the feature extraction methods are explained below.

GPS sensor The APP triggers a reading event every 10 seconds. A GPS measurement $\widehat{g} = (\widehat{x}, \widehat{v}, \widehat{h}, \widehat{\sigma}^x, \widehat{t})$ is extracted for each GPS reading, and it contains: $\widehat{t}$, the measurement time, in seconds; $\widehat{x} = (\widehat{x}_{lat}, \widehat{x}_{lon})$, a pair of GPS horizontal coordinates in WGS84 format; $\widehat{\sigma}^x$, the standard deviation of the horizontal error in $\widehat{x}$, in meters; $\widehat{v}$, a speed measurement, in km/h; $\widehat{h}$, a heading measurement, that is the angle to the north direction, from 0 to 359, clockwise. Sometimes, the GPS sensor fails to measure the speed and heading values for a measurement, and it reports the exact same values as in the previous measurement. In this case, the speed and heading values of the measurement have to be calculated. If we denote two consecutive GPS measurements as $\widehat{y}_1$ and $\widehat{y}_2$ respectively, Figure 2 shows how to calculate $\widehat{v}_2$ and $\widehat{h}_2$.

Bluetooth sensor The APP configures the BT sensor to scan for nearby BT devices every 180 seconds. Each scan returns a list of nearby BT devices with their unique identifiers (MAC addresses). Nowadays, many people carry BT-enabled personal electronic devices, such as smartphones and tablets. These devices are visible to each other if, they are in a range of approximately 10 meters; and they do not move out of this range for a short time, which is 1.92 seconds in average (Naya, Noma & Kogure 2005). The number of nearby visible BT devices varies with the context. In public transport, people

are more compact in the vehicle, and they are stationary relative to each other. Hence a smartphone has a higher chance to observe more BT devices than in private transport. Therefore, we utilized the information about nearby BT devices in differentiating public/private transport context. A measurement $(\widehat{b}, \widehat{t})$ is extracted from each BT scan, and $\widehat{b}$ is equal to 1 if there is at least one BT device nearby, and 0 otherwise. It is also associated with a time stamp $\widehat{t}$.

Accelerometer sensor Accelerometer readings provide motion status of the phone user. It has been proposed in the literature to use them to detect the transport mode of the traveler (e.g. Reddy et al. 2009). A N95 smartphone is embedded with a 3-axis accelerometer with the sensitivity of $\pm 2G$. An accelerometer reading is a triplet that contains the accelerations measured from 3 axes. The unit of the acceleration is $\frac{1}{280} m/s^2$, in which 280 is a normalization factor. The APP triggers an accelerometer reading event every 120 seconds. Every reading event lasts for 10 seconds in a frequency of $40Hz$. Therefore, it returns 400 accelerometer readings. Table 1 gives an example of data returned from a reading event. The first two columns indicate the index and the time stamp of each piece of reading. The last three columns are elements of the triplets measured from the three axes.

We assume random orientation of the smartphones, and calculate the acceleration for each reading by taking the 2-norm of the triplet. Due to the high frequency of recording noisy acceleration data, an aggregation method is needed here. The aggregation takes a time resolution of 2 seconds, and split the 10 seconds data into 5 equal time windows. This aggregation technique is generally used in practice in order to reduce the noise in the acceleration data (e.g., Reddy et al. (2009) use 1 second as the time resolution). In each time window, a measurement $(\widehat{a}, \widehat{t})$ is generated with $\widehat{a}$ as the mean of the accelerations in this time window. The measurement time $\widehat{t}$ is set to be the middle of the time window. Consequently, 5 accelerometer measurements are generated by each ACCEL reading event.

2.3 Measurements sequence from a trip

The APP records data from independent sensors with a pre-defined schedule. We assume that the data have been preprocessed so that we have access to all the measurements recorded during a trip, and store them in a chronologically ordered sequence $(\widehat{y}_1, \ldots, \widehat{y}_T)$, which is abbreviated as $\widehat{y}_{1:T}$[2], where T is the total number of measurements.

[2]This paper deals with data sequences, and the notation follows this abbreviation convention throughout the paper.

The entire sequence is composed of 3 subsequences: the GPS, the BT, and the ACCEL. For example, we denote all the GPS measurements as $(\widehat{g}_1, \widehat{g}_2, \ldots, \widehat{g}_I)$, where I is the total number of GPS.

Since only GPS provides valuable geographical location information, the measurements sequence $\widehat{y}_{1:T}$ is processed such that the first and the last measurements are GPS. All BT and ACCEL measurements recorded before the first GPS or after the last GPS are excluded. In $\widehat{y}_{1:T}$, if different types of measurements have the same time stamp, the order is set to be BT, ACCEL, and then GPS. If two GPS measurements have a large time gap, they do not provide reliable location information to BT and ACCEL data observed between them. Therefore, we decide to discard BT and ACCEL data if the time gap is large, and 20 seconds is chosen as the time threshold. The reason is explained in Section 4.3 in details.

Some sensor data (dataset A) with annotated transport modes are used to calibrate sensor measurement models (Section 3) and a speed distribution for each transport mode (Section 4). These data are collected from 3 smartphone users while they are traveling with various transport modes. The true transport modes of the travels are known. The numerical experiments in Section 6 use measurements sequences (dataset B) that are collected from 2 smartphone users while they are traveling in urban and outskirt areas. More details about the data will be provided in the corresponding sections.

3 Sensor measurement models

In this section, measurement models are defined to represent the sensors' operations in a multimodal transport network context. A measurement model has the form $\Pr(\widehat{y}|\mathbf{x}, t)$, where the state variable $\mathbf{x} = (x, m)$ is the position of the phone carrier in the network, and $\widehat{y}$ denotes a sensor measurement collected at time $\widehat{t}$. Conditional on the state $\mathbf{x}$, the measurement $\widehat{y}$ is derived for a value of t equal to the time stamp $\widehat{t}$ of the measurement. Therefore, the model can be denoted as $\Pr(\widehat{y}|\mathbf{x})$. The rest of this section defines a sensor measurement model for each type of measurement, i.e. GPS, BT and ACCEL.

3.1 GPS measurement model

The GPS measurement model proposed here focuses on the location only, and is therefore denoted by $\Pr(\widehat{x}|\mathbf{x})$. It is an extension of the measurement model proposed by Bierlaire et al. (2010). In this multimodal context, it is assumed that the horizontal coordinates are independent

of the transport mode,

$$\Pr(\widehat{x}|\mathbf{x}) = \Pr(\widehat{x}|x) = \exp\left(-\frac{\|x-\widehat{x}\|_2^2}{2\widehat{\sigma}^2}\right), \tag{1}$$

where $\|x-\widehat{x}\|_2$ calculates the distance (in meters) between the recorded coordinates $\widehat{x}$ and the coordinates x in the transport network; the variance $\widehat{\sigma}^2$ is approximated by $\widehat{\sigma}^2 = \sigma^2_{\text{network}} + \widehat{\sigma}^2_x$, where $\sigma_{\text{network}} = 30m$ is the standard deviation of the horizontal error in network data (for more detailed discussions, see Bierlaire et al. 2010).

3.2 BT measurement model

As discussed in Section 2.2, we assume that the BT measurement $\widehat{b}$ only depends on whether the transport mode is public or private, then we have:

$$\Pr(\widehat{b}|\mathbf{x}) = \Pr(\widehat{b}|m) = \begin{cases} \Pr(\widehat{b}|m \in \text{PT}) & \text{if } m \text{ is PT} \\ \Pr(\widehat{b}|m \notin \text{PT}) & \text{if } m \text{ is non-PT} \end{cases}$$

where $\text{PT} = \{\text{bus}, \text{metro}\}$ denotes the set of public transport modes. The PT and non-PT models are based on empirical distributions. They are calibrated from the annotated BT data of dataset A, and reported in Table 2. The number of measurements used for calibration is 869 for PT and 1826 for non-PT respectively. We observe that the chance of observing a BT device is higher in public transport.

3.3 ACCEL measurement model

Acceleration merely provides information about the transport mode, so we assume it to be independent of the location. As for the BT data, we derive a model based on an empirical distribution. Then we have $\Pr(\widehat{a}|\mathbf{x}) = f_a(\widehat{a}|m)$, where $f_a(\widehat{a}|m)$ denotes the probability density function of the ACCEL measurement for mode m. Furthermore, we assume that motor-based transport modes (including car, bus and metro) have the same pattern of acceleration. Then we calibrate a probability density function for walk, bike and motor-based transport modes respectively, and denote them as $f_a(\widehat{a}|\text{walk})$, $f_a(\widehat{a}|\text{bike})$ and $f_a(\widehat{a}|\text{motor})$.

For each density function, a finite mixture of normal is used to model the distribution of the acceleration measurement:

$$f_a(\widehat{a}) = \sum_{j=1}^{J} w_j \phi(\mu_j, \sigma_j^2). \tag{2}$$

The following parameters need to be estimated: J, the number of normal components; w_j, the proportion of component j ($w_j \geq 0$, $\sum_{j=1}^{J} w_j = 1$); μ_j and σ_j^2, the mean and the variance of the normal distribution $\phi(\mu_j, \sigma_j^2)$. These parameters are estimated from the annotated ACCEL data of dataset A. The estimation technique is described by Park, Zhang & Lord (2010) where the same method is applied to model the heterogeneous speed data. A *R* package *mixAK* is used for the estimation (Komárek 2009). The histograms of the ACCEL measurements and the predictive densities are drawn in Figure 3. Table 3 reports the parameter estimates (standard error is given in parentheses). On the header, the figure below each mode indicates the amount of measurements used for the calibration. The gravity $1G$ corresponds to 280 in the ACCEL measurement, so deviation from 280 means acceleration caused by the smartphone's movement. Acceleration less than gravity is usually caused by vertical movements. We can observe distinct patterns from the distributions. *Walk* is the least stable movement status since it has a higher chance to observe a high acceleration value. *Bike* has a peak near $1G$, which means that the movement is quite stable with little acceleration. *Motor* has a peak centered at less than $1G$, which depicts vertical movements caused by the road condition (e.g., bumps and uphills) and the usage of the phone in the vehicle.

4 Smartphone measurement model

In this section, an integrated smartphone measurement model is proposed to combine the sensor measurement models in a unified framework. This smartphone measurement model $\Pr(\widehat{y}_{1:T}|t_{1:T}, p)$ is intended to calculate the likelihood of observing all the smartphone measurements $\widehat{y}_{1:T}$ on a multimodal path p at time $t_{1:T}$ respectively. We assume that the time is recorded without error. Therefore, the model will return a non zero probability only when the sequence $t_{1:T}$ exactly matches the sequence of time stamp $\widehat{t}_{1:T}$ in the data.

4.1 Derivation of the smartphone measurement model

The derivation of the smartphone measurement model builds on the procedure described by Bierlaire et al. (2010). In this paper, we focus on the main differences introduced by the multimodal context and the integration of various sensors.

The measurement equation is decomposed as:

$$\Pr(\widehat{y}_{1:T}|t_{1:T},p) \quad = \Pr(\widehat{y}_1|t_1,p)\prod_{k=2}^{T}\Pr(\widehat{y}_k|\widehat{y}_{1:k-1},t_{1:k},p), \tag{3}$$

where $\Pr(\widehat{y}_k|\widehat{y}_{1:k-1},t_{1:k},p)$ is the conditional probability for observing $\widehat{y}_k$, and is calculated iteratively. The complex dependency in the sequentially observed measurements is modeled by this conditional probability. In order to simplify its derivation, we assume that the observation of measurement $\widehat{y}_k$ on path p at time t_k only depends on the previous observation. Then the conditional probability for observing $\widehat{y}_k$ simplifies to

$$\Pr(\widehat{y}_k|\widehat{y}_{1:k-1},t_{1:k},p) \approx \Pr(\widehat{y}_k|\widehat{y}_{k-1},t_k,p), \tag{4}$$

For the first measurement, which is always a GPS measurement by construction, we derive

$$\Pr(\widehat{y}_1|t_1,p) \quad = \textstyle\int_{\mathbf{x}_1\in p}\Pr(\widehat{y}_1|\mathbf{x}_1)\Pr(\mathbf{x}_1|t_1,p)d\mathbf{x}_1 \tag{5}$$

$$= \textstyle\int_{\mathbf{x}_1\in p}\Pr(\widehat{x}_1|\mathbf{x}_1)\Pr(\mathbf{x}_1|t_1,p)d\mathbf{x}_1, \tag{6}$$

where the probability $\Pr(\mathbf{x}_1|t_1,p)$ captures a prior knowledge of the initial position of the device. If nothing is known, it can for instance be defined as $\frac{1}{L_p}$ where L_p is the length of path p. For each subsequent observation $k \geq 2$, we have

$$\Pr(\widehat{y}_k|\widehat{y}_{k-1},t_k,p) = \int_{\mathbf{x}_k\in p}\Pr(\widehat{y}_k|\mathbf{x}_k)\Pr(\mathbf{x}_k|\widehat{y}_{k-1},t_k,p)d\mathbf{x}_k, \tag{7}$$

where $\Pr(\mathbf{x}_k|\widehat{y}_{k-1},t_k,p)$ represents the prior probability that the device is at (multimodal) position $\mathbf{x}_k$ at time t_k given the last observed measurement $\widehat{y}_{k-1}$, and can be derived by:

$$\Pr(\mathbf{x}_k|\widehat{y}_{k-1},t_k,p) = \int_{\mathbf{x}_{k-1}\in p}\Pr(\mathbf{x}_k|\mathbf{x}_{k-1},\widehat{t}_{k-1},t_k,p)\Pr(\mathbf{x}_{k-1}|\widehat{y}_{k-1},p)d\mathbf{x}_{k-1}, \tag{8}$$

where $\Pr(\mathbf{x}_{k-1}|\widehat{y}_{k-1},p)$ is the posterior distribution of $\mathbf{x}_{k-1}$ from last iteration,

$$\Pr(\mathbf{x}_{k-1}|\widehat{y}_{k-1},p) = \frac{\Pr(\widehat{y}_{k-1}|\mathbf{x}_{k-1})}{\int_{\mathbf{x}_{k-1}\in p}\Pr(\widehat{y}_{k-1}|\mathbf{x}_{k-1})d_{\mathbf{x}_{k-1}}}. \tag{9}$$

Putting everything together, we have

$$\begin{aligned}&\Pr(\widehat{y}_k|\widehat{y}_{k-1},\widehat{t}_{k-1},t_k,p)\\ &= \frac{\int_{\mathbf{x}_k\in p}\int_{\mathbf{x}_{k-1}\in p}\Pr(\widehat{y}_{k-1}|\mathbf{x}_{k-1})\Pr(\mathbf{x}_k|\mathbf{x}_{k-1},\widehat{t}_{k-1},t_k,p)\Pr(\widehat{y}_k|\mathbf{x}_k)d_{\mathbf{x}_{k-1}}d_{\mathbf{x}_k}}{\int_{\mathbf{x}_{k-1}\in p}\Pr(\widehat{y}_{k-1}|\mathbf{x}_{k-1})d_{\mathbf{x}_{k-1}}}.\end{aligned} \tag{10}$$

There are two kinds of essential components in this equation. One is the sensor measurement models, $\Pr(\widehat{y}_1|\mathbf{x}_1)$, $\Pr(\widehat{y}_{k-1}|\mathbf{x}_{k-1})$ and $\Pr(\widehat{y}_k|\mathbf{x}_k)$, which are already described in Section 3; the other is the travel model $\Pr(\mathbf{x}_k|\mathbf{x}_{k-1}, \widehat{t}_{k-1}, t_k, p)$, which we define next.

4.2 Travel model

The travel model with the form

$$\Pr(\mathbf{x}_k|\mathbf{x}_{k-1}, t_{k-1}, t_k, p) \tag{11}$$

essentially predicts the position $\mathbf{x}_k = (x_k, m_k)$ at time t_k, given that the state at time t_{k-1} is $\mathbf{x}_{k-1} = (x_{k-1}, m_{k-1})$, and the smartphone user is traveling along path p. There are several ways of implementing the travel model, for instance, via a traffic simulator or real-time traffic information. In this paper, we extend the empirical model proposed by Bierlaire et al. (2010) to multimodal context. It is based on the speed distribution for each transport mode.

4.2.1 Speed distributions

Researchers have been using speed profiles to infer transport modes (e.g. Liao, Patterson, Fox & Kautz 2007, Zheng et al. 2008, Reddy et al. 2009, Bohte & Maat 2009). Studies have also been performed on estimating the speed profiles of transport modes (e.g. Knoblauch, Pietrucha & Nitzburg 1996, Thompson, Rebolledo, Thompson, Kaufman & Rivara 1997).

A speed distribution for car has been estimated by Bierlaire et al. (2010). The distribution is assumed to be a mixture of a negative exponential and a log-normal. The first is designed to capture the period when the traveler is stopped, or traveling at low speed before or after that stop. The second is designed to capture the traveler moving at regular speed. In this paper, this method is adapted to estimate a speed distribution $f_v(v|m)$ for each transport mode. Speed measurements from dataset A are used for the estimation. And the probability density function for mode m is written as:

$$f_v(v|m) = w_m \lambda_m e^{-\lambda_m v} + (1 - w_m) \frac{1}{v\sqrt{2\pi\tau_m^2}} e^{-\frac{(\ln v - \mu_m)^2}{2\tau_m^2}}. \tag{12}$$

Our data analysis shows that a mixture of negative exponential and normal fits better for walk. The distribution for walk is therefore

$$f_v(v|\text{walk}) = w_{\text{walk}} \lambda_{\text{walk}} e^{-\lambda_{\text{walk}} v} + (1 - w_{\text{walk}}) \frac{1}{\sqrt{2\pi\tau_{\text{walk}}^2}} e^{-\frac{(v - \mu_{\text{walk}})^2}{2\tau_{\text{walk}}^2}}. \tag{13}$$

The parameters to be estimated are: w_m, the weight for the mixture; λ_m, the scale parameter of the negative exponential distribution; μ_m, the location parameter of the normal and log-normal distributions respectively; τ_m the scale parameter of the normal and log-normal distributions respectively. Figure 4 shows the normalized histograms of the recorded speed data and the estimated speed distributions for all modes. Table 4 reports the parameters estimated by maximum likelihood, as well as the amount of data that is used for the estimation. The standard error for each parameter estimate is given in parentheses.

4.2.2 Derivation of the travel model

A multimodal path differs from a unimodal path in that there are possible mode changes along a path. Therefore, there are two situations that need to be considered in deriving the travel model: the presence or absence of a virtual mode transfer arc between $\mathbf{x}_{k-1}$ and $\mathbf{x}_k$ along p.

If there is no mode change between $\mathbf{x}_{k-1}$ and $\mathbf{x}_k$. The smartphone carrier travels from $\mathbf{x}_{k-1}$ to $\mathbf{x}_k$ along path p with the same mode $m_k = m_{k-1}$. Then the probability density function of the travel model (11) can also be written as

$$f_x(x_k|x_{k-1}, t_{k-1}, t_k, m_k, p), \tag{14}$$

which predicts the next location x_k of the unimodal (m_k) travel along path p since the previous location x_{k-1}. We assume that the travel speed follows the speed distribution of the transport mode m_k being used in this uni-modal travel segment, then we have the following model:

$$f_x(x_k|x_{k-1}, t_{k-1}, t_k, m_k, p) = f_v(\frac{d_p(x_{k-1}, x_k)}{t_k - t_{k-1}}|m_k), \tag{15}$$

where $d_p(x_{k-1}, x_k)$ calculates the distance from x_{k-1} to x_k on path p; so that $\frac{d_p(x_{k-1},x_k)}{t_k-t_{k-1}}$ calculates the travel speed; and the probability density function f_v is given by Equation (12) or (13).

If there are mode changes between $\mathbf{x}_{k-1}$ and $\mathbf{x}_k$. Considering the fact that the GPS data are recorded every 10 seconds, we assume that it is not possible to have more than one mode change in such a short time. The mode change between $\mathbf{x}_{k-1}$ and $\mathbf{x}_k$ is represented by a virtual arc on p, associated with coordinates x_c. We denote upstream node of the virtual arc by $\mathbf{x}_c^- = (x_c, m_{k-1})$ and the downstream node by $\mathbf{x}_c^+ = (x_c, m_k)$. The time at which the mode

change happens is unknown and denoted by $t_c \in [t_{k-1}, t_k]$. Then, we have the following model:

$$\Pr(\mathbf{x}_k|\mathbf{x}_{k-1}, t_{k-1}, t_k, p) = \int_{t_c=t_{k-1}}^{t_k} \Pr(t_c|\mathbf{x}_{k-1}, t_{k-1}, p) \Pr(\mathbf{x}_k|\mathbf{x}_{k-1}, t_c, t_k, p) dt_c, \quad (16)$$

The two probabilities in the RHS of Equation (16) describe the two unimodal travel segments before and after the mode change. The first predicts the mode change time t_c; the second predicts the position $\mathbf{x}_k$ at time t_k given the mode change time t_c. Following the derivation of Equation (15), we also assume that the travel speed of each segment follows the speed distribution of the corresponding transport mode. Then, they can be re-written as:

- $\Pr(t_c|\mathbf{x}_{k-1}, t_{k-1}, p) = f_v(\frac{d_p(x_{k-1}, x_c)}{t_c - t_{k-1}}|m_{k-1})$,
- $\Pr(\mathbf{x}_k|\mathbf{x}_{k-1}, t_c, t_k, p) = f_v(\frac{d_p(x_c, x_k)}{t_k - t_c}|m_k)$.

4.3 Computing integrals

The above formulations involve a lot of integrals along path p with the form of $\int_{\mathbf{x}\in p} f(\mathbf{x})d\mathbf{x}$. In order to save computation time, Bierlaire et al. (2010) define a Domain of Data Relevance (DDR) of each GPS point as a physical area nearby. Then, the domain of the integral is truncated to the part of the path that is inside the DDR.

Obviously, this simplification method only works for GPS data, because other data do not contain location information. In this paper, the domain of integral for BT and ACCEL measurements is illustrated in Figure 5. For each BT or ACCEL measurement $\widehat{y}_k$, its previous and next GPS measurements are denoted as $\widehat{y}_{k^{g-}}$ and $\widehat{y}_{k^{g+}}$ ($t_{k^{g-}} \leq t_k \leq t_{k^{g+}}$). Since measurements are observed sequentially, $\widehat{y}_k$'s state $\mathbf{x}_k \in p$ has to be downstream of $\mathbf{x}_{k^{g-}}$ and upstream of $\mathbf{x}_{k^{g+}}$. Then, the domain of integral for $\mathbf{x}_k$ only includes the domains of integral for $\mathbf{x}_{k^{g-}}$ and $\mathbf{x}_{k^{g+}}$ (part 1&2 in Figure 5), plus the part of p that connects $\mathbf{x}_{k^{g-}}$ and $\mathbf{x}_{k^{g+}}$ (part 3). This definition highly relies on the two adjacent GPS measurements. If the GPS measurements happen to have a large time gap, they do not provide reliable location information for BT and ACCEL data observed between them. Therefore, as mentioned in Section 2.3, the BT and ACCEL measurements observed between them are discarded. For the implementation of the DDR of GPS measurements and the integral, we refer to Bierlaire et al. (2010) for more details.

5 Candidate path generation

The probabilistic measurement model $\Pr(\widehat{y}_{1:T}|t_{1:T}, p)$ calculates the likelihood of observing measurements $\widehat{y}_{1:T}$ on a given path p at time $t_{1:T}$. Given a set of candidate paths P, it can be further used to infer how likely p is to be the true path:

$$q(p) = \frac{\Pr(\widehat{y}_{1:T}|t_{1:T}, p)\Pr(p)}{\sum_{p' \in P}\Pr(\widehat{y}_{1:T}|t_{1:T}, p')\Pr(p')}, \tag{17}$$

This path probability can be used as a score function in traditional deterministic map-matching algorithms (e.g. Schuessler & Axhausen 2009b) for determining which path is the true one. Considered as the prior probability, $\Pr(p)$ represents how likely p would be traveled without having the smartphone data. It actually models the smartphone user's route choice behavior. If no route choice model is available, the distribution can be assumed to be uniform for instance.

This section focuses on the generation of P. Note that, because we assume that the time tags are measured without error, the values of $t_{1:T}$ are taken directly from the data $\widehat{t}_{1:T}$. We propose a multimodal candidate path generation algorithm as an extension of a unimodal algorithm developed by Bierlaire et al. (2010). This algorithm has special features compared to the conventional map-matching and transport mode inference algorithms:

- The algorithm builds the physical path and the transport modes simultaneously.
- Smartphone data recorded from a trip are not required to be preprocessed into several unimodal segments.
- Transport networks also contribute to the inference of the transport mode, especially in differentiating PT and non-PT modes.

Usually, a map-matching algorithm takes two sources of information: location data, and transport networks data. In this algorithm, although BT and ACCEL measurements do not contain significant location information for generating path candidates, they are implicitly used in the process that eliminates paths according to the path probability (17). The output is a set of candidate multimodal paths. For each path, the likelihood (3) of observing the smartphone measurements on it, and the probability (17) that it is the true path are also calculated.

The algorithm iterates over the sequence of GPS measurements $\widehat{g}_{1:I}$. At each iteration i, it generates a set of candidate paths P_i that are matched to the sequence of all measurements (including BT and ACCEL) up to $\widehat{g}_i$. In the next iteration $i+1$, each path is extended

from its end node, and downstream segments are appended in order to map the new measurements up to the next GPS $\widehat{g}_{i+1}$. In fact, this iterative method connects the DDR of the GPS points to build candidate paths. Practically, the number of candidate paths grows exponentially because each DDR is relatively large with about $100m$ radius (Bierlaire et al. 2010). Therefore, heuristics are proposed to reduce the computational burden. The result from the last iteration I is the final output of the algorithm. The pseudo-code is briefly described as Algorithm 1. Detailed explanations of some steps are given as follows:

9. At iteration i, the path extension process is carried out only when the GPS point $\widehat{g}_i$ is far enough away from $\widehat{g}_{i'}$, where i' corresponds to the last iteration when a path extension happened, and $100m$ is chosen as the distance threshold. Otherwise, the traveler is considered to be immobile, and a path extension is not necessary.

15. The path extension from end node n takes place in each unimodal network G_m, if n appears in G_m or connects to G_m with a virtual arc (mode change). A new path candidate p_{new} is created by joining the current path candidate $p \in P_{i'}$ with the newly discovered downstream segment (see line 22). The transport mode m of the downstream segment is the mode of G_m. It can be different from the mode of the last arc on p. In other words, a mode change is allowed to happen at the connecting node n, which is the end node of p.

16. Each transport mode has a speed limit. For example, walk is not expected to have a speed over $18km/h$. If the observed speed $\widehat{v}_i$ of the GPS exceeds the maximum speed of a transport mode m, the corresponding unimodal transport network G_m is neglected. This is mainly designed to neglect walk and bike networks when the GPS is in fact observed from higher speed motor modes, hence to reduce the amount of irrelevant paths as candidates. The maximum speed for walk and bike is set to be $18km/h$ and $40km/h$ respectively, while no constraint is imposed to motor modes. These values correspond to 99% percentile in the speed data of dataset A.

18. Shortest path trees are used to link the DDRs of adjacent GPS points. For the sake of computational efficiency, the shortest path trees are bounded. The leaf nodes of a bounded shortest path tree are the first nodes detected by the Dijkstra algorithm that violates the bound. The bound is the same as in Bierlaire et al. (2010). It is based on an assumption about the maximum possible speed of the traveler within the time interval $[t_{i'},\ t_i]$.

Algorithm 1: Path extension procedure in iteration i

Input: The smartphone measurements sequence $\widehat{y}_{1:T}$ with GPS subsequence $\widehat{g}_{1:I}$

Input: The underlying multimodal transportation network G with multiple unimodal networks G_m, $m \in \{\text{walk}, \text{bike}, \text{car}, \text{bus}, \text{metro}\}$.

Result: A set of candidate paths P_I.

```
// Deal with the first GPS point.
```

$P_1 \leftarrow$ empty set of paths;

for *each arc* $a \in A$ **do**

  $DDR_1 \leftarrow$ the DDR of the first GPS measurement;

  if a *intersects* DDR_1 **then**

    include a as a partial path in P_1;

$i' \leftarrow 1$: the temporary index for processed GPS;

for $i \leftarrow 2$ *to* I **do**

```
// Iterative path extension process.
```

  if $\|\widehat{x}_i - \widehat{x}_{i'}\| > 100m$ **then**

    $i' \leftarrow i$;

    foreach $p \in P_{i'}$ **do**

      if p *intersects* DDR_i **then**

        include p in P_i;

      $n \leftarrow$ the end node of p;

      foreach *unimodal network* G_m **do**

        if $\widehat{v}_i \leq$ *the maximum speed of mode* m **then**

          $spt \leftarrow$ a bounded shortest path tree rooted at n in G_m ;

          foreach *link* $a \in spt$ **do**

            if a *intersects* DDR_k **then**

              $sp \leftarrow$ shortest path connecting p and a;

              $p_{new} \leftarrow$ join p, sp and a;

              include p_{new} in P_i;

    limit the size of P_i;

In our experiments, the bound is defined by $1.5(t_i - t_{i'})\widehat{v}_{\max}$, where $\widehat{v}_{\max}$ is the maximum speed value among the observed GPS speeds $\widehat{v}_{i'}$ and $\widehat{v}_i$, and the speed value calculated from the coordinates: $\|\widehat{x}_i - \widehat{x}_{i'}\|_2/(t_i - t_{i'})$. The factor 1.5 is a safety margin to minimize the risk of missing a relevant observation.

24. The path elimination procedure is designed to speed up the algorithm by eliminating less relevant branches. It eliminates unreasonable paths deterministically according to various criteria. The deterministic elimination procedure includes:

    1. We assume that walk is necessary for mode changes. Therefore, if a path has a mode change without walk involved, it is eliminated.
    2. A path with loops is considered to be unreasonable, hence is excluded, unless the loops involve walk.
    3. A path might be too long to be consistent with the observed travel time approximated by $t_I - t_1$. The mean travel speed $\bar{v}_m$ for each mode m is taken from the speed data of dataset A. Then the mean travel time for a path can be calculated by summing up the mean travel time $\frac{L_a}{\bar{v}_{m_a}}$ for each arc a, where m_a is the mode of arc a and L_a is the length of the arc. We assume the lower bound of a path's travel time as half of the mean travel time. If the observed travel time is lower than the lower bound, the path is considered too long to be realistic, and removed.

    Clearly, more behavioral rules could be considered here, possibly involving a calibrated behavior model.

    In order to control the complexity of the algorithm, the number of paths generated at each iteration should be reasonably small. For example, Marchal, Hackney & Axhausen (2005) and Schuessler & Axhausen (2009b) suggest to maintain 30 paths at each iteration for unimodal map matching. We use a random sampling procedure to select paths according to the path probability (17). Since the algorithm is multimodal, we decide to maintain more paths, but not more than 60 paths in our experiments. The random selection procedure includes three steps.

    1. Randomly draw some paths from P_i according to the path probability (17). In our experiments, 20 paths are selected.
    2. Let $P_i^1 \subseteq P_i$ denote the set of paths with the least mode changes. Then, randomly sample some paths from P_i^1 according to the path probability (17). Before the random sampling, the probabilities are normalized such that they

sum up to one for the paths in P_i^1. In this step, paths with the least mode changes are favored because they are more behaviorally reasonable. In our experiments, 10 paths are selected in this step.

3. The likelihood that the GPS measurement is observed on a is defined:

$$\Pr(\widehat{x}|a) = \int_{x \in a} \Pr(\widehat{x}|x) \Pr(x|a) dx = \frac{1}{L_a} \int_{x \in a} \Pr(\widehat{x}|x) dx. \tag{18}$$

A_{im} is defined as the set of arcs that intersect with DDR_i and have the transport mode m. For each mode m, we sample some arcs according to the likelihood (18) (as in Step2, the normalization of the likelihood is required before the random sampling). In our experiments, 5 arcs for each mode are selected. For each sampled arc a, we denote $P_{\text{ia}} \subseteq P_i$ as the set of paths that go via a and have the least mode changes. We then apply a similar random sampling procedure as in Step 2 on P_{ia}, but only to draw one path. In this step, the sampled paths go through different arcs with different modes that intersect with DDR_i. Therefore, this step ensures sufficient variability in the generated paths.

If a trip is unimodal and the mode is known, the algorithm can be used to only identify the physical path. It is simply accomplished by supplying the unimodal transport network of the known mode. Since this technique is essentially unimodal map-matching, it is denoted as Algorithm-U, while the original multimodal algorithm is denoted as Algorithm-M. In the next section, the results generated by Algorithm-U with the correct transport mode will be used as the benchmark when we analyze the mode inference performance of Algorithm-M.

6 Numerical experiments

The proposed method is implemented as a software package in C++. It reads smartphone data and OSM network data as inputs, and produces probabilistic map-matching results. In this section, numerical experiments are performed with smartphone data collected in different circumstances. Some examples are first illustrated with map visualization to gain an intuitive impression of the results. Then, numerical analyses focus on the performance in inferring the modes. The contributions of BT and ACCEL data are also analyzed.

6.1 Result illustration

Some common trip patterns are chosen for the illustration, including bike, car, and public transport with changes. Using information from dataset A, the main transport modes for each trip are known while the exact path is unknown.

The first example in Figure 7(a) shows a complex multimodal trip with metro→walk→bus→walk. The total travel time is 20 minutes, and there are 91 GPS measurements generated, with 8 BT, and 395 ACCEL. The background network is shown in gray lines, while a generated path is drawn with color. According to the smartphone user who provided the data, this path resembles the trip that he made. The graph without background network shows the same path. The red arrow shows the direction of the trip. There are 43 paths generated by the multimodal map-matching algorithm (Algorithm-M). The measurement log likelihood $\ln(\Pr(\widehat{y}_{1:T}|t_{1:T}, p))$ for each path is plotted in Figure 6, and the x-axis shows the id of each path. We notice that some paths have much higher log likelihood than the others. The path 22 drawn in Figure 7(a) gains the highest log likelihood (-347.9).

The differences of the generated paths show the uncertainty of the result. On one hand, the uncertainty is due to the imprecision of the smartphone data and the network. On the other hand, the uncertainty mainly belongs to the end of the trip, since we notice that the generated paths mainly differ at the end of them. This can be explained by the mechanism of the smartphone measurement model. The model utilizes the dependency between adjacent measurements (see Equation 4). Each measurement in fact provides information to identify its upstream trajectory. The end of a trip always gains less information since it has less (or none) downstream measurements. We focus on the differences of the paths by showing the end of them in Figure 7(b). Graph 1 shows path 22's end; Graph 2 shows path 23's end, which has a different destination (log likelihood -348.7); Graph 3 shows path 14, of which a part is identified as car (log likelihood -384.0); Graph 4 shows path 40 with its end identified as bike (log likelihood -381.9).

The second example in Figure 8 shows a car trip. All the generated 30 paths are drawn in the figure, and they greatly overlap with each other. Except for the uncertainty of the trip end, there is also uncertainty (marked by a circle) due to the data noise and the density of the network.

The third example in Figure 9 shows a trip with bike as the main mode. There are 33 paths generated, the left graph draws a path with the highest log likelihood -117.7. The same path without background network is drawn in the top right graph. The end of the path is identified as walk because the smartphone user is entering a park-

ing place. The bottom right graph shows another representative path, which gains a little lower log likelihood −118.0. The differences between two paths are highlighted in circles.

In these examples, the paths with the highest likelihoods are chosen for illustration purpose only. In practice, we suggest to carry the uncertainty in the application, together with the associated probability. For example, in route choice modeling, the probabilistic path observations from the map-matching results can be used with network-free method (Bierlaire et al. 2010).

6.2 Performance analysis

In order to gain more systematic understanding of the performance of the algorithm, analysis with more data is provided. The analysis focuses on the most important aspects of the method proposed in this paper: the identification of the modes, and the usage of various kinds of data. For the sake of convenience, we extract from dataset A data sequences that are known to have one single mode. 36 data sequences are used for the analysis. The transport mode, the travel time, the number of GPS, BT and ACCEL measurements for each data sequence is given in the left part of Table 5.

Since each data sequence has a known transport mode, Algorithm-U with the known mode can be applied to generate unimodal paths that have the correct transport mode. Algorithm-M are then applied, and the map-matching results (path sets) are denoted as follows:

P^0: Algorithm-U is applied to only GPS data, with known mode.

P^1: Algorithm-M is applied to only GPS data.

P^2: Algorithm-M is applied to GPS and BT data, if BT data are available.

P^3: Algorithm-M is applied to all data, if ACCEL data are available.

Since P^0 has the correct transport mode, hence it is served as the benchmark. The performance of Algorithm-M with different data is evaluated by comparing P^1, P^2, P^3 against P^0. We expect that P^1, P^2 and P^3 are similar to P^0, if Algorithm-M correctly identifies the paths and the modes. In order to compare the path sets, we first define quantitative similarity indicators.

Similarity indicators

First, the overlapping indicator $O(p, P)$ is defined to measure how much a path p overlaps with all the paths in a path set P:

$$O(p, P) = \sum_{a \in p} \frac{L_a}{L_p} \sum_{p' \in P} q(p') \delta_{ap'}, \tag{19}$$

where $\delta_{ap'}$ is a dummy variable, valued 1 if path p' contains arc a, and 0 otherwise; L_a and L_p are the lengths of arc a and path p respectively; $q(p')$ is the path probability (17). This definition is inspired by the concept of Path Size used in route choice modeling to measure how an alternative overlaps with other paths in the choice set (see Ben-Akiva & Bierlaire 2003) . This overlapping indicator is valued between 0 and 1, and can be roughly understood as the average proportion of the path p overlapping with all paths in P. When p is the same as any path in P, then the overlap is total and $O(p, P) = 1$; when p does not overlap with any path in P at all, $O(p, P) = 0$.

Then $S(P', P)$ is defined to compare another path set P' against P,

$$S(P', P) = \sum_{p \in P'} q(p) O(p, P). \tag{20}$$

This definition is inspired by the similarity indicator proposed by Bierlaire et al. (2010). We include here the path probability $q(p)$, which weights the importance of each path. S is also valued between 0 and 1. When all paths in both P and P' are the same, $S(P', P) = 1$; when all paths are distinct without any overlap, $S(P', P) = 0$. If $P' = P$, $S(P, P)$ in fact calculates the similarity of the paths in the same set. When P is a map-matching result, $S(P, P)$ indicates the level of the uncertainty in the result. The higher the similarity, the lower the uncertainty. For example, $S(P, P)$ for the first example in Section 6.1 is 0.967, for the second is 0.956, while for the third is lower 0.854 because more uncertainty is observed.

For the comparison of the different results, we select P^0 as benchmark, and analyze the values $S^0 = S(P^0, P^0)$, $S^1 = S(P^1, P^0)$, $S^2 = S(P^2, P^0)$, $S^3 = S(P^3, P^0)$. The uncertainty of the unimodal matching result S^0 tells the degree of the data noise and the density of the network. S^1, S^2, S^3 are expected to have a high value, but not higher than S^0.

Analysis

The similarity indicators for all trips are reported in Table 5. A empty cell means that the corresponding data is not available, hence no result

is generated. S^2 is empty when BT data are unavailable, S^3 is empty when ACCEL data are unavailable.

We first notice that all S^0 have high value with low uncertainty in the results. The value is 0.921 in average. Since the uncertainty is mainly due to the error of the GPS data and the density of the transport network, S^0 for walk data is lower because the walk network is usually denser.

When Algorithm-M is applied with the multimodal network, we have $S^1, S^2, S^3 < S^0$, because the algorithm is not aware of the true mode and there is a chance of mis-identifying it. However, in the majority of the cases, S^1 is close to S^0, and the average of S^1 is 0.757, which is 82.2% of the average of S^0. Considering the complexity of the multimodal network and the sparsity of the GPS data, Algorithm-M achieves quite high accuracy in the transport mode inference. We observe some exceptional cases (case 1, 8, 25, and 28), where S^1 has very low value. There are mainly due to two reasons. First, in case 1, 25 and 28, the GPS data are too sparse, therefore the measurements do not provide enough information to find out the correct mode. Indeed, in case 1, there are only 12 GPS measurements observed in 479 seconds. Second, in case 8, the data are observed when the bus was running slowly in peak hour in the city center. Therefore, the chance of identifying the mode as bike increases. In these two cases, some generated paths have very strange mode change behavior, such as, using both bike and car in 10 minutes. We believe that if an appropriate route choice behavior model is incorporated in the candidate path generation algorithm, such paths will be less favored by the algorithm.

By comparing S^1 among different modes, we observe that non-PT cases have high values, because people do not follow the PT lines during the entire trip when they use private mode. Hence the chance of mis-identifying the mode as public transport (bus and metro) is low. In this situation, the transport network helps in identifying the mode. From another perspective, if a route choice behavior model can consider the fact that private mode travel does not follow PT lines, the results could further be improved.

In 12 cases where BT data are available, the average of S^2 (0.888) is greater than the average of S^1 (0.858). In 22 cases where ACCEL data are available, the average of S^3 (0.826) is greater than the average of S^1 (0.751). Therefore, in general, the additional BT and ACCEL data contribute to the accuracy of the results. Additional ACCEL data are particularly helpful when S^1 has very low value (case 8, 25 and 28). In some cases, although there are drops in S^3 with additional data, the values are still acceptable. Still, ACCEL data need to be used more carefully. We notice that ACCEL data are special when the vehicle

is traveling at low speed, because the vehicle is usually accelerating or decelerating then. This information can be used to improve the ACCEL measurement model in the future.

The numerical experiments with real smartphone data show that the proposed multimodal map-matching algorithm performs well in identifying the multimodal paths from the smartphone data. BT and ACCEL data also contribute to the identification of the transport mode.

7 Conclusions

This paper proposes a probabilistic method to infer the path and the modes of a trip from smartphone data. A smartphone measurement model is derived to calculate the likelihood that a smartphone would have generated a sequence of measurements while traveling on a multimodal path. It is based on a structural travel model that captures the dynamic of the smartphone user's state in the transport network, and sensor measurement models that capture the sensors' operation. This smartphone measurement model synthesizes information available from various sensors, such as GPS, BT and ACCEL.

An algorithm is developed to generate candidate paths from the smartphone data. This algorithm identifies the physical path and the modes of a trip simultaneously. Hence, the transport network information is also utilized to identify the transport modes of a trip. Data recorded from a multimodal trip do not need to be divided into unimodal travel segments. The result of the algorithm is a set of candidate multimodal paths, along with a probability for each being the true one.

The visualized examples show that the results are intuitively reasonable, and the measurement likelihood values are realistic and meaningful. A complex multimodal trip example shows the capability of the algorithm in dealing with mode changes. Numerical analysis shows the performance of the algorithm in identifying the transport modes. Apart from the most useful GPS data, BT and ACCEL also contribute in identifying the transport mode.

Future works involve more investigations on the usage of BT and ACCEL data. They need to be used more carefully, because they do not contain any location information, and highly rely on the adjacent GPS measurements to have prior information about where they are observed. More sophisticated BT measurement model can be considered. In particular, we may want to capture the fact that walk might happen in a crowded place where BT devices are observed. In this case the location and time of the day should play roles in the BT measurement model. Also, the measurement variable can be defined as the

number of nearby devices in order to utilize more information from the BT data. Apart from the mean, more features of the ACCEL data can also be used, such as the variation. Traffic model can be more advanced, and the timetable of public transport can be used when available. Also, if a route choice model is available in the candidate path generation algorithm, the results will be further improved. Finally, the probabilistic map-matching results will be used to estimate multimodal route choice behavior.

Ackowledgments

This research is supported by the Swiss National Science Foundation grant 200021/131998 *Route choice models and smart phone data*. Nokia Research Center in Lausanne, and IDIAP Switzerland have helped in providing smartphone data access.

References

Ben-Akiva, M. & Bierlaire, M. (2003). Discrete choice models with applications to departure time and route choice, *in* R. Hall (ed.), *Handbook of Transportation Science, Second Edition*, Kluwer Academic Publishers, Boston/Dordrecht/London, pp. 7–37.

Bierlaire, M., Chen, J. & Newman, J. (2010). Using location observations to observe routing for choice models, *Proceedings of the 89th Annual Meeting of Transportation Research Board*, Washington, D.C., USA.

Bohte, W. & Maat, K. (2009). Deriving and validating trip purposes and travel modes for multi-day {GPS}-based travel surveys: A large-scale application in the {N}etherlands, *Transportation Research Part C: Emerging Technologies* **17**(3): 285–297.

González, M. C., Hidalgo, C. A. & Barabási, A.-L. (2008). Understanding individual human mobility patterns., *Nature* **453**(7196): 779–82.
URL: *http://dx.doi.org/10.1038/nature06958*

Kiukkonen, N., Blom, J., Dousse, O., Gatica-Perez, D. & Laurila, J. (2010). Towards rich mobile phone datasets: Lausanne data collection campaign, *ICPS 2010: The 7th International Conference on Pervasive Services*, Berline.

Knoblauch, R., Pietrucha, M. & Nitzburg, M. (1996). Field Studies of Pedestrian Walking Speed and Start-Up Time, *Transportation*

Research Record: Journal of the Transportation Research Board **1538**(-1): 27–38.
URL: *http://dx.doi.org/10.3141/1538-04*

Komárek, A. (2009). A new R package for Bayesian estimation of multivariate normal mixtures allowing for selection of the number of components and interval-censored data, *Computational Statistics & Data Analysis* **53**(12): 3932–3947.

Kwapisz, J., Weiss, G. & Moore, S. (2010). Activity Recognition using Cell Phone Accelerometers, *Proceedings of the Fourth International Workshop on Knowledge Discovery from Sensor Data*, pp. 10–18.
URL: *http://storm.cis.fordham.edu/ gweiss/papers/sensorKDD-2010.pdf*

Liao, L., Patterson, D., Fox, D. & Kautz, H. (2007). Learning and inferring transportation routines, *Artificial Intelligence* **171**(5-6): 311–331.
URL: *http://linkinghub.elsevier.com/retrieve/pii/S0004370207000380*

Marchal, F., Hackney, J. & Axhausen, K. W. (2005). Efficient map matching of large Global Positioning System data sets: Tests on speed-monitoring experiment in Zurich, *Transportation Research Record: Journal of the Transportation Research Board* **1935**: 93–100.

Naya, F., Noma, H. & Kogure, K. (2005). Bluetooth-based Indoor Proximity Sensing for Nursing Context Awareness, *Ninth IEEE International Symposium on Wearable Computers (ISWC'05)* pp. 212–213.
URL: *http://ieeexplore.ieee.org/lpdocs/epic03/wrapper.htm?arnumber=1550816*

Park, B.-J., Zhang, Y. & Lord, D. (2010). Bayesian mixture modeling approach to account for heterogeneity in speed data, *Transportation Research Part B: Methodological* **44**(5): 662–673.
URL: *http://linkinghub.elsevier.com/retrieve/pii/S0191261510000196*

Reddy, S., Burke, J., Estrin, D., Hansen, M. & Srivastava, M. (2009). Determining transportation mode on mobile phones, *Wearable Computers, 2008. ISWC 2008. 12th IEEE International Symposium on*, IEEE, pp. 25–28.
URL: *http://ieeexplore.ieee.org/xpls/abs_ all.jsp?arnumber=4911579*

Schuessler, N. & Axhausen, K. (2009a). Processing Raw Data from Global Positioning Systems Without Additional Information, *Transportation Research Record: Journal of the Transportation Research Board* **2105**: 28–36.

Schuessler, N. & Axhausen, K. W. (2009b). Map-matching of {GPS} Traces on High-resolution Navigation Networks Using the Multiple Hypothesis Technique, *Working paper* .

Tam, M. L. & Lam, W. H. (2008). USING AUTOMATIC VEHICLE IDENIFICATION DATA FOR TRAVEL TIME ESTIMATION IN HONG KONG, *Transportmetrica* **4**(3): 179–194.
URL: *http://dx.doi.org/10.1080/18128600808685688*

Thompson, D. C., Rebolledo, V., Thompson, R. S., Kaufman, a. & Rivara, F. P. (1997). Bike speed measurements in a recreational population: validity of self reported speed., *Injury prevention : journal of the International Society for Child and Adolescent Injury Prevention* **3**(1): 43–5.
URL: *http://www.pubmedcentral.nih.gov/articlerender.fcgi?artid=1067763&tool=pmcentrez&*

Zhang, L., Dalyot, S., Eggert, D., Sester, M., Ikg, G., Hannover, L. U. & De, M. S. (2008). MULTI-STAGE APPROACH TO TRAVEL-MODE SEGMENTATION AND CLASSIFICATION OF GPS TRACES, *World* pp. 87–93.

Zheng, Y., Li, Q., Chen, Y., Xie, X. & Ma, W.-y. (2008). Understanding Mobility Based on GPS Data, *Tenth International Conference on Ubiquitous Computing*, number 49, pp. 312–321.

Tables

Table 1: Acceleration data returned from a reading event

index	time stamp	x-axis	y-axis	z-axis
1	1272678293.03	15.0	-15.0	-324.0
2	1272678293.05	21.0	-15.0	-324.0
3	1272678293.09	21.0	-15.0	-329.0
...	...	...	...	...
398	1272678302.91	21.0	-15.0	-324.0
399	1272678302.94	15.0	-10.0	-319.0
400	1272678302.95	15.0	-15.0	-324.0

Table 2: Probability density mass of $\widehat{b}$ for PT and non-PT

$\Pr(\widehat{b}\|m)$	$\widehat{b}=0$	$\widehat{b}=1$
$m \in$ PT	0.81	0.19
$m \notin$ PT	0.60	0.40

Table 3: Parameter estimates for ACCEL distributions

	walk 4501	bike 11924	motor 11801
J	3	4	4
w_1	$7.773e-01$ $(2.782e-02)$	$2.106e-01$ $(5.727e-02)$	$1.922e-01$ $(4.496e-03)$
μ_1	$3.152e+02$ $(1.202e+00)$	$2.929e+02$ $(3.038e+00)$	$2.647e+02$ $(9.726e-02)$
σ_1	$2.206e+01$ $(7.589e-01)$	$9.907e+00$ $(1.327e+00)$	$3.496e+00$ $(7.860e-02)$
w_2	$2.151e-01$ $(2.814e-02)$	$3.217e-01$ $(5.676e-02)$	$7.537e-01$ $(8.748e-03)$
μ_2	$3.712e+02$ $(2.938e+00)$	$2.766e+02$ $(1.063e+00)$	$3.102e+02$ $(2.324e-01)$
σ_2	$1.879e+01$ $(1.711e+00)$	$8.039e+00$ $(4.633e-01)$	$1.333e+01$ $(2.061e-01)$
w_3	$7.668e-03$ $(3.924e-03)$	$2.047e-01$ $(2.102e-02)$	$4.450e-02$ $(4.700e-03)$
μ_3	$3.983e+02$ $(4.307e+01)$	$3.284e+02$ $(3.289e-01)$	$2.864e+02$ $(2.463e-01)$
σ_3	$1.059e+02$ $(2.843e+01)$	$6.411e+00$ $(4.536e-01)$	$2.633e+00$ $(1.872e-01)$
w_4	-	$2.631e-01$ $(4.501e-02)$	$9.626e-03$ $(5.186e-03)$
μ_4	-	$3.163e+02$ $(2.055e+00)$	$3.545e+02$ $(1.213e+01)$
σ_4	-	$2.075e+01$ $(9.360e-01)$	$2.158e+01$ $(5.339e+00)$

Table 4: Parameter estimates for speed distributions

mode	measurements	w_m	λ_m	μ_m	τ_m
walk	9350	0.46 (0.01)	0.20 (0.00)	4.41 (0.03)	1.51 (0.03)
bike	11899	0.39 (0.01)	0.09 (0.00)	2.88 (0.00)	0.30 (0.00)
metro	1142	0.52 (0.02)	0.17 (0.01)	3.51 (0.03)	0.43 (0.02)
bus	1669	0.48 (0.07)	0.13 (0.03)	3.16 (0.05)	0.46 (0.02)
car	2069	0.20 (0.03)	0.12 (0.03)	3.76 (0.03)	0.62 (0.02)

Table 5: Numerical comparisons of results

	mode	time	GPS	BT	ACCEL	S^0	S^1	S^2	S^3
1	bus	479	12	0	19	0.99	0.07	-	0.15
2	bus	399	40	0	25	0.98	0.93	-	0.93
3	bus	234	24	1	11	0.96	0.64	0.65	0.93
4	bus	499	47	0	23	0.98	0.81	-	0.98
5	bus	255	24	0	23	0.96	0.96	-	0.97
6	bus	412	42	0	41	0.97	0.94	-	0.86
7	bus	417	39	2	34	0.98	0.98	0.98	0.98
8	bus	479	35	0	7	0.98	0.27	-	0.50
9	car	229	20	0	23	0.97	0.95	-	0.96
10	car	180	16	0	0	0.95	0.87	-	-
11	car	241	23	0	23	0.92	0.91	-	0.90
12	car	229	24	0	0	0.93	0.93	-	-
13	bike	290	29	0	0	0.91	0.55	-	-
14	bike	289	27	0	0	0.80	0.68	-	-
15	bike	313	32	0	0	0.93	0.80	-	-
16	bike	369	38	1	23	0.83	0.76	0.77	0.76
17	bike	1153	115	0	98	0.96	0.89	-	0.81
18	bike	1021	100	4	73	0.97	0.95	0.95	0.77
19	metro	892	62	1	34	0.99	0.99	0.99	0.97
20	metro	560	34	1	23	0.99	0.77	0.82	0.85
21	metro	259	16	0	0	0.98	0.94	-	-
22	metro	409	33	1	23	0.98	0.99	0.98	0.99
23	metro	594	49	2	40	0.99	0.95	0.96	0.96
24	metro	716	38	2	0	0.96	0.80	0.91	-
25	metro	601	16	0	20	0.97	0.13	-	0.89
26	metro	449	39	0	20	0.99	0.98	-	0.99
27	metro	230	22	0	23	0.95	0.76	-	0.94
28	metro	579	7	0	10	0.98	0.08	-	0.48
29	walk	1269	114	0	0	0.88	0.71	-	-
30	walk	719	62	0	0	0.65	0.58	-	-
31	walk	659	47	0	0	0.76	0.80	-	-
32	walk	998	97	5	0	0.93	0.90	0.88	-
33	walk	240	21	0	0	0.72	0.59	-	-
34	walk	359	27	1	0	0.80	0.75	0.73	-
35	walk	488	38	0	0	0.85	0.84	-	-
36	walk	490	35	2	26	0.83	0.81	0.77	0.61

Figure Captions

Figure 1. A multimodal network and a multimodal path

Figure 2. Calculate speed and heading

Figure 3. ACCEL distributions for walk, bike, and motor

Figure 4. Speed distributions of 6 transport modes

Figure 5. Integral domain for BT or ACCEL measurement $\widehat{y}_k$

Figure 6. Measurement log likelihood for paths

Figure 7. A multimodal trip

Figure 8. A car trip

Figure 9. A bike trip

Figures

Figure 1: A multimodal network and a multimodal path

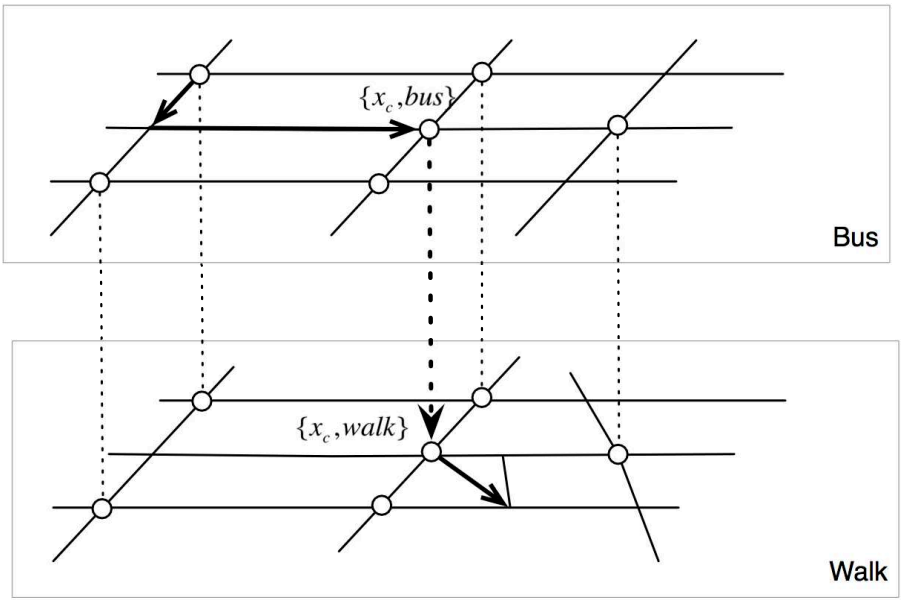

Figure 2: Calculate speed and heading

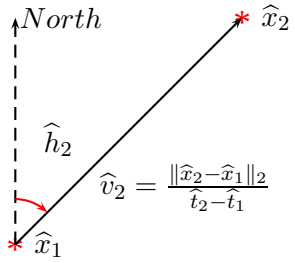

Figure 3: ACCEL distributions for walk, bike, and motor

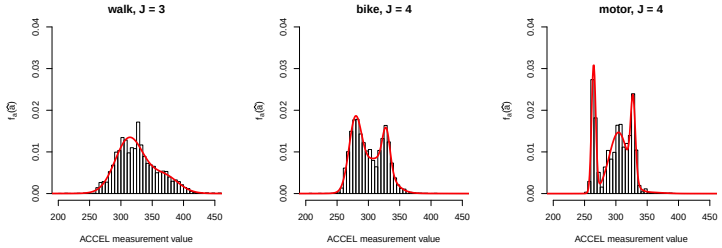

Figure 4: Speed distributions of 6 transport modes

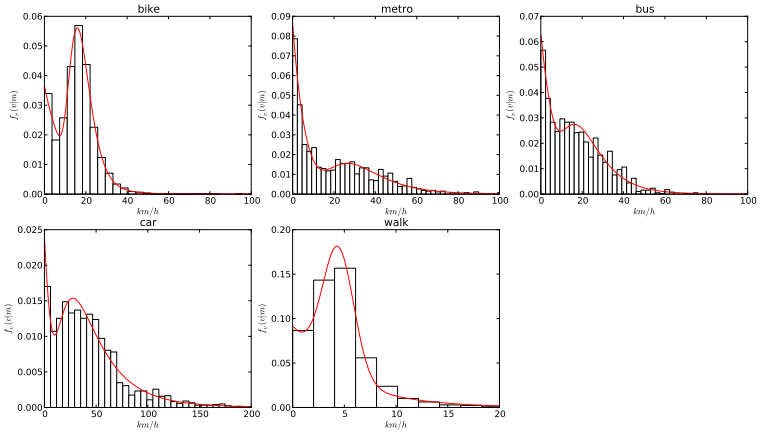

Figure 5: Integral domain for BT or ACCEL measurement $\widehat{y}_k$

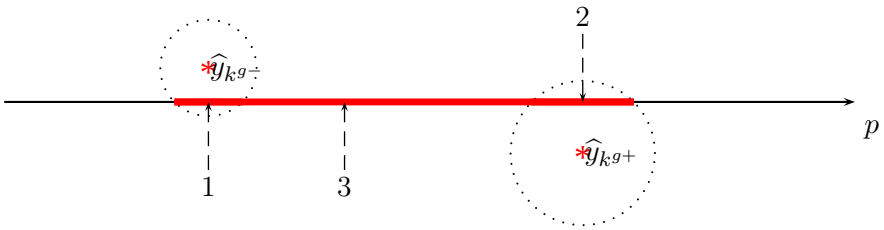

Figure 6: Measurement log likelihood for paths

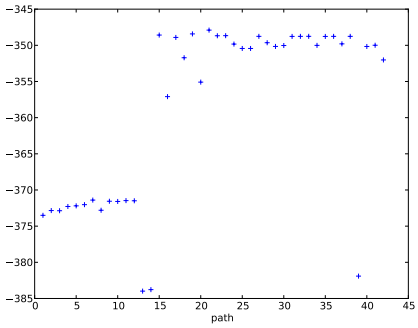

Figure 7: A multimodal trip

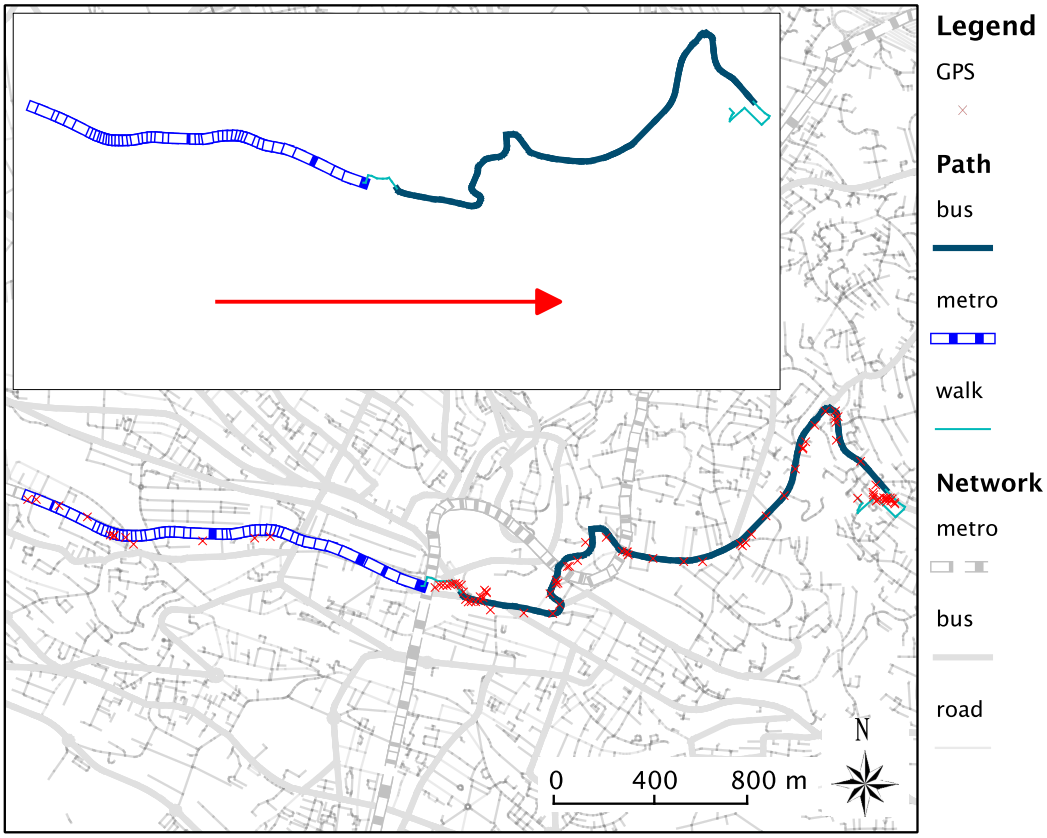

(a) Data and a generated path

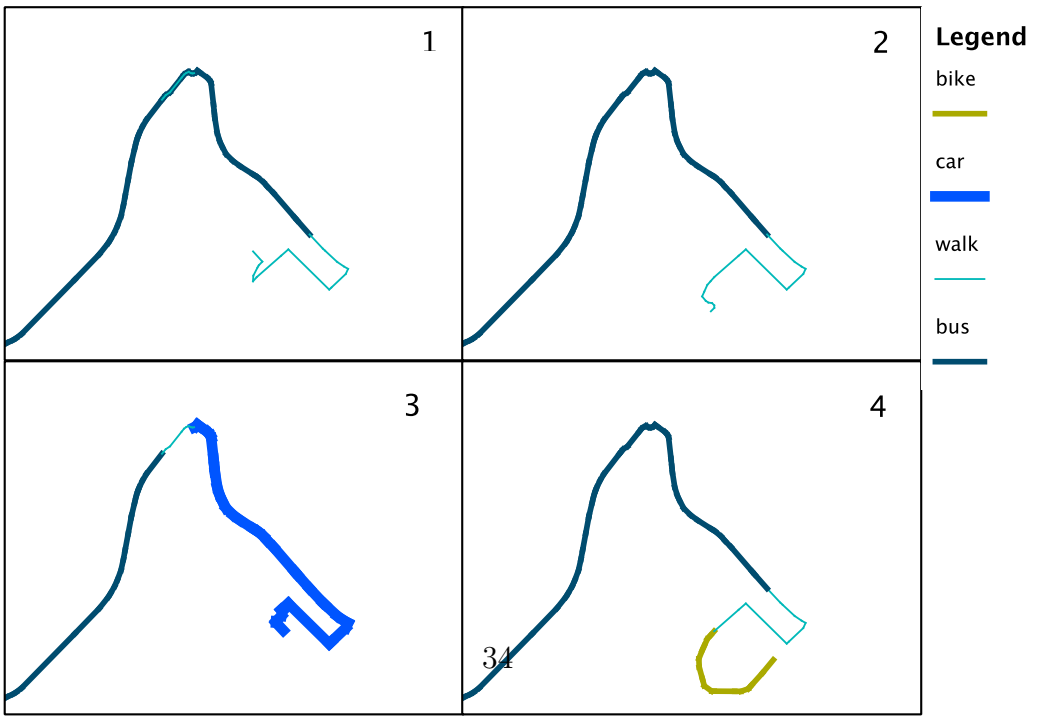

(b) Trip end uncertainty

Figure 8: A car trip

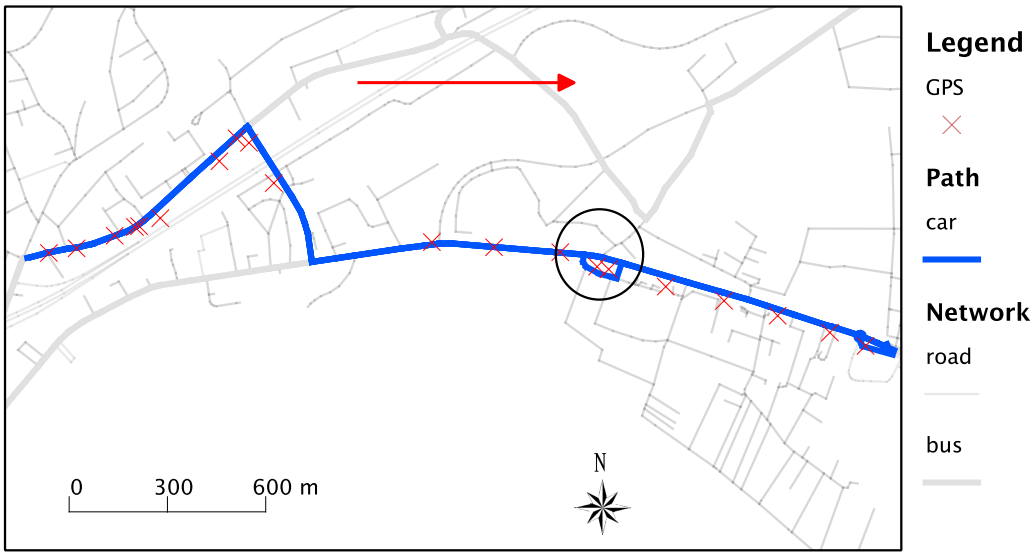

Figure 9: A bike trip